Rapid Communications

Nonadiabatic electron dynamics in time-dependent density functional theory at the cost of adiabatic local density approximation

D. R. Gulevich and Ya. V. Zhumagulov
ITMO University, St. Petersburg 197101, Russia

A. Vagov
Theoretische Physik III, Universität Bayreuth, 95440 Bayreuth, Germany
and ITMO University, St. Petersburg 197101, Russia

V. Perebeinos
Department of Electrical Engineering, University at Buffalo, The State University of New York, Buffalo, New York 14260, USA
and ITMO University, St. Petersburg 197101, Russia

(Received 30 August 2019; published 13 December 2019)

We propose a computationally efficient approach to account for the nonadiabatic effects in time-dependent density functional theory (TDDFT) based on a representation of the frequency-dependent exchange-correlation kernel as a response of a set of damped oscillators. The requirements to computational resources needed to implement our approach do not differ from those of the standard real-time TDDFT in the adiabatic local density approximation. Thus, our result offers an exciting opportunity to take into account temporal nonlocality and memory effects in calculations with TDDFT in quantum chemistry and solid state physics for unprecedentedly low costs.

DOI: 10.1103/PhysRevB.100.241109

Time-dependent density functional theory (TDDFT) [1] has recently become a standard tool for studying electronic excitations in molecules, atomic clusters, and solid state (see reviews [2–5] and books [6,7]). Its real-time formulation based on solving the time-dependent Kohn-Sham (TDKS) equation allows one to not only obtain the linear excitation spectra, but to also study nonlinear dynamics under arbitrary time-dependent perturbations [8–22].

Implementations of real-time TDDFT available in the standard density functional theory packages [23–27] utilize the adiabatic approximation, which neglects the frequency dependence of the exchange-correlation (xc) kernels introduced to capture exchange interactions and correlation effects of the electron subsystem. Significant progress in the development of TDDFT beyond the adiabatic approximation has been made by appreciating that the current $\mathbf{j}(\mathbf{r}, t)$ rather than the density $n(\mathbf{r}, t)$ could be used as the main variable in the xc functional [28,29]. The arising theory is known as the time-dependent current-density functional theory (TDCDFT) [7]. Based on the homogeneous electron gas as a reference system, Vignale and Kohn were able to construct a dynamical but spatially local functional for TDCDFT [30]. The idea has been cast in the form of hydrodynamic equations [30–33] and a theory of deformations in the comoving Lagrangian frame [34–36].

The interest in developing xc functionals beyond the adiabatic local density approximation (ALDA) using a number of alternative approaches [37–45] is driven by the demand from the optimal quantum control problems [46–48], studies of multiple and double excitations in molecules [49–54] and exciton physics [55–60]. The Vignale-Kohn nonadiabatic functional has so far been applied to metals [61], molecules [62], and semiconductors [63], although, only in the linear response. The nonlinear regime requires solving the TDKS equation which was done for quantum wells [64,65] and simple molecules [66,67]. The major obstacle limiting applications of the real-time TDCDFT is that the TDKS equation at each instant depends on values of the velocity field $\mathbf{u}(\mathbf{r}, t) = \mathbf{j}(\mathbf{r}, t)/n(\mathbf{r}, t)$ in the entire past evolution. The need to store and process all the previous history makes numerical implementation of real-time TDCDFT impractical for realistic systems.

In this work, we show how to bypass this computational difficulty by presenting an efficient approach with the demand for computational resources similar to that for the real-time TDDFT-ALDA. Our method opens up an exciting opportunity to take into account nonadiabatic effects in TDDFT calculations in quantum chemistry and solid state physics with only a marginal rise of the computing cost. The proposed approach is based on the following representation of frequency-dependent xc kernels:

$$f_{xc}(n,\omega) = f_{xc}(n,\infty) + \frac{1}{2}\sum_{m=1}^{M}\left[\frac{C_m(n)\,p_m(n)}{\omega - p_m(n)} - \frac{C_m^*(n)\,p_m^*(n)}{\omega + p_m^*(n)}\right], \quad (1)$$

where poles $p_m(n)$ and weights $C_m(n)$ are complex functions of electron density n. The imaginary part of the poles satisfies the condition $\mathrm{Im}\, p_m(n) < 0$, which follows from causality of the response, whereas the real part of the weights is subjected

to the sum rule

$$\sum_{m=1}^{M} \mathrm{Re}\, C_m(n) = f_{xc}(n,\infty) - f_{xc}(n,0). \tag{2}$$

Although the kernel in Eq. (1) may comprise infinitely many terms, in practice, there is always a finite number of dominant contributions which fully define the response. Furthermore, because the nonadiabatic kernels are known only approximately, a sufficiently accurate model can be constructed with a few dominant terms in Eq. (1). As we demonstrate below, even a kernel comprising a single term in the sum (1) is capable of reproducing dynamics of interacting electron systems on a par with the significantly more complex models [68–75].

The form of Eq. (1) allows one to draw an analogy with the classical models of optical susceptibility [76]. Indeed, the representation Eq. (1) can be seen as a response of a set of damped Lorentz oscillators with the density-dependent natural frequencies $\omega_m(n) = |p_m(n)|$, damping parameters $-2\,\mathrm{Im} p_m(n)$, and oscillator strengths $\mathrm{Re} C_m(n)$. Thus, one can interpret Eq. (1) as an effective interaction of the electron subsystem with a set of independent oscillators responsible for the temporal nonlocality of the TDKS equation. We refer to this model as the *oscillator model for xc kernels* (OMXC).

The OMXC has the following key properties which make it particularly useful for practical implementation of the real-time TDDFT beyond the adiabatic approximation:

(i) Both real and imaginary parts of the OMXC kernels are defined by explicit complex function of the complex frequency. In contrast, the standard parametrizations [68–75] of the imaginary part of xc kernels require a careful analytic continuation into the lower complex half-plane [77] and evaluation of complicated integrals in order to find the real part [78].

(ii) Imaginary and real parts of the quantity $f_{xc}(n,\omega) - f_{xc}(n,\infty)$ given by Eq. (1) satisfy the Kramers-Kronig relations.

(iii) When transformed to the time domain, Eq. (1) yields an explicit function of time which satisfies the causality.

(iv) A simple analytic structure of Eq. (1) admits an intuitive interpretation providing insight into the underlying physics. In some cases, positions of the poles $p_m(n)$ can be guessed from the relevant physical processes and, vice versa, location of the poles may explain the physics behind the nonadiabatic xc kernels.

(v) Most importantly, the OMXC enables one to construct highly efficient numerical schemes for the real-time TDCDFT. In what follows, we will elaborate the foundations for the efficient implementations of real-time TDCDFT. We will focus on three-dimensional (3D) electron systems, although our approach can be applied to two-dimensional systems equally well.

The bottleneck of the real-time TDCDFT in the Vignale-Kohn approximation is evaluation of the xc viscoelastic stress tensor [31]:

$$\sigma_{ij}^{xc}(\mathbf{r},t) = \int_0^t dt' \Big\{ \eta_{xc}(\bar{n}, t-t') \Big[\partial_i u_j(\mathbf{r},t') + \partial_j u_i(\mathbf{r},t') - \frac{2}{3} \nabla\cdot\mathbf{u}(\mathbf{r},t')\delta_{ij} \Big] + \zeta_{xc}(\bar{n}, t-t') \nabla\cdot\mathbf{u}(\mathbf{r},t')\delta_{ij} \Big\}, \tag{3}$$

where $\mathbf{u}(\mathbf{r},t)$ is the velocity field and we assume that at $t<0$ the electron system is in the ground state. The average density $\bar{n}$ which enters Eq. (3) can be evaluated at either t or t' as the difference between $n(\mathbf{r},t)$ and $n(\mathbf{r},t')$ can be neglected within the Vignale-Kohn approximation [30,64,79]. The time-dependent kernels $\eta_{xc}(n,t)$ and $\zeta_{xc}(n,t)$ are the Fourier transforms of the complex viscosity coefficients

$$\eta_{xc}(n,\omega) = \frac{in^2}{\omega+i0} f_{xc}^T(n,\omega),$$
$$\zeta_{xc}(n,\omega) = \frac{in^2}{\omega+i0}\left[f_{xc}^L(n,\omega) - \frac{4}{3} f_{xc}^T(n,\omega) - \frac{d^2\epsilon_{xc}(n)}{dn^2} \right], \tag{4}$$

where the label L (T) stands for the longitudinal (transverse) component of the kernel, and $\epsilon_{xc}(n)$ is the xc energy density of the homogeneous electron gas. The standard approach [64,65,79] of solving the TDKS equation in the real-time TDCDFT is to calculate the time integral for the stress tensor in Eq. (3) directly using the time-dependent kernels $\eta_{xc}(n,t)$ and $\zeta_{xc}(n,t)$. However, this brute-force approach puts an enormous load on the computational resources. Indeed, to propagate the TDKS equation, one needs to store the previous evolution of the velocity field, while using it in evaluations of the integrals (3) at every time step. To keep the computation feasible, one is forced to introduce a cutoff for the memory depth to prevent an unbound rise of the computer memory and computing time [65,80]. Often, one resorts to the instantaneous (Markovian) approximation [66,67] by neglecting the very dependence on the evolution history.

With the help of the OMXC one can significantly reduce both the computing time and the extensive load on the computer memory without any compromise for the treatment of nonadiabatic effects. In contrast to the instantaneous approximation, our method enables one to take into account arbitrary long memory of the evolution. The main idea is to avoid evaluation of the costly time integrals in Eq. (3) and of the inverse Fourier transforms of Eq. (4) by introducing auxiliary dynamical equations associated with individual oscillators of the OMXC. Substituting Eq. (1) for both longitudinal and transverse components of the xc kernel in Eq. (4), yields

$$\eta_{xc}(n,\omega) = \frac{in^2}{2} \sum_{m=0}^{M} \left[\frac{C_m^T(n)}{\omega - p_m^T(n)} + \frac{C_m^{T*}(n)}{\omega + p_m^{T*}(n)} \right] \tag{5}$$

and

$$\zeta_{xc}(n,\omega) = -\frac{4}{3}\eta_{xc}(n,\omega) + \frac{in^2}{2} \sum_{m=0}^{M} \left[\frac{C_m^L(n)}{\omega - p_m^L(n)} + \frac{C_m^{L*}(n)}{\omega + p_m^{L*}(n)} \right], \tag{6}$$

where we introduced the terms at $m=0$, such that $p_0^{L,T}(n) = -i0$ and

$$C_0^L(n) = f_{xc}^L(n,0) - \frac{d^2\epsilon_{xc}(n)}{dn^2}, \quad C_0^T(n) = f_{xc}^T(n,0). \tag{7}$$

Transforming (5) and (6) to the time domain and substituting to Eq. (3), we reduce the expression for xc stress tensor to

$$\sigma_{ij}^{xc}(\mathbf{r},t) = n^2 \sum_{r=L,T}\sum_{m=0}^{M} \mathrm{Re}\int_0^t C_m^r(\bar{n}) \times e^{-ip_m^r(\bar{n})(t-t')}\mu_{ij}^r(\mathbf{r},t')dt', \tag{8}$$

where we introduced

$$\mu_{ij}^L(\mathbf{r},t) = \nabla\cdot\mathbf{u}(\mathbf{r},t)\delta_{ij},$$
$$\mu_{ij}^T(\mathbf{r},t) = \partial_i u_j(\mathbf{r},t) + \partial_j u_i(\mathbf{r},t) - 2\nabla\cdot\mathbf{u}(\mathbf{r},t)\delta_{ij}. \tag{9}$$

Employing the ambiguity of the Vignale-Kohn approximation [30], according to which $\bar{n}$ in Eq. (8) is either $n(\mathbf{r},t)$ or $n(\mathbf{r},t')$, we can rewrite the expression for the xc stress tensor in the form

$$\sigma_{ij}^{xc}(\mathbf{r},t) = n^2 \sum_{r=L,T}\sum_{m=0}^{M} \mathrm{Re}\left\{C_m^r[n(\mathbf{r},t)]\mathcal{M}_{mij}^r(\mathbf{r},t)\right\}, \tag{10}$$

where $\mathcal{M}_{mij}^r(\mathbf{r},t)$ are memory variables which satisfy the evolution equation

$$\frac{\partial}{\partial t}\mathcal{M}_{mij}^r(\mathbf{r},t) = \mu_{ij}^r(\mathbf{r},t) - ip_m^r[n(\mathbf{r},t)]\,\mathcal{M}_{mij}^r(\mathbf{r},t), \tag{11}$$

with the initial condition $\mathcal{M}_{mij}^r(\mathbf{r},0) = 0$.

The memory variables $\mathcal{M}_{mij}^r(\mathbf{r},t)$ are associated with individual OMXC oscillators and carry information about previous evolution of the system, holding, in principle, an infinite memory of $\mu_{ij}^r(\mathbf{r},t)$. Equations (10) and (11), which have to be solved in addition to the TDKS equation, eliminate the need of both storing the past evolution and evaluating the integrals in Eq. (3). Thus, this approach lays the foundation for highly efficient numerical schemes, where all memory effects are taken into account by propagating auxiliary time-local differential equations (cf. numerical schemes used in the Josephson physics [81,82]).

It is evident that given $p_m^r(n)$ and $C_m^r(n)$, the computational overhead of finding $\sigma_{ij}^{xc}(\mathbf{r},t)$ according to Eqs. (10) and (11) is minor compared to solving the TDKS equation itself. Therefore, the only factor which limits the computational efficiency of this approach is evaluations of $p_m^r(n)$ and $C_m^r(n)$ from the electron density $n(\mathbf{r},t)$. However, such computational costs are comparable to evaluation of the ALDA exchange-correlation potential. Moreover, the numerical effort can be further reduced, if the expressions for $p_m^r(n)$ and $C_m^r(n)$ involve powers of the electron density, such as $n^{1/3}$ or similar. In this case, their values can be reused from evaluation of the adiabatic component of the xc vector potential. Thus, the performance of the real-time TDCDFT based on the proposed approach (TDCDFT-OMXC) promises to be comparable to that of the standard real-time TDDFT-ALDA. As a proof of concept, we will construct a simple OMXC kernel of the form (1) and apply it to the benchmark problem of collective intersubband excitations in a quantum well [77,79].

To derive the single-oscillator OMXC kernel, we proceed as follows. We will focus on the longitudinal component $f_{xc}^L(n,\omega)$ which we will need in our calculation of dynamics of intersubband excitations, although the same arguments apply

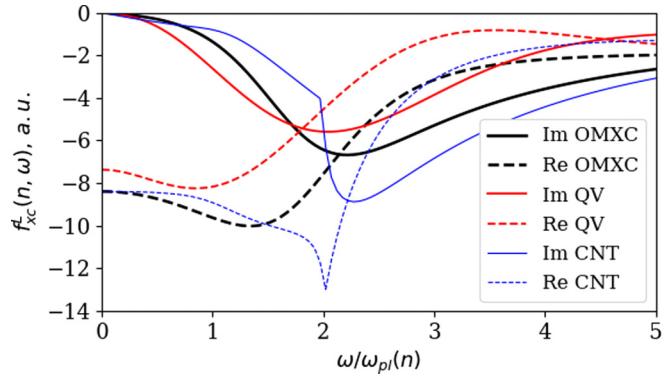

FIG. 1. The single-oscillator OMXC kernel (thick black lines) given by Eq. (12). Parametrizations of Qian-Vignale [75] (QV, red lines) and Conti-Nifosi-Tosi [72,74] (CNT, blue lines) for 3D electron gas are also shown. All kernels are evaluated at the electron density n which corresponds to the Wigner-Seitz radius $r_s = 3$ bohrs.

to the transverse component $f_{xc}^T(n,\omega)$ as well. Using the prediction that $\mathrm{Im}f_{xc}^L(n,\omega)$ has a peak at twice the plasmon frequency $\omega_{pl}(n)$ [71,72], we set $|p_1^L(n)| = 2\,\omega_{pl}(n)$. Despite the theoretical efforts [72,74,75], the peak width $-2\,\mathrm{Im}p_m^L(n)$ at the double plasmon frequency is much less known. The perturbation theory [72,74,83] predicts the low-frequency side of the double plasmon peak to scale with the plasma frequency $\omega_{pl}(n)$. Thus, for the single-pole OMXC kernel we take

$$\left|p_1^L(n)\right| = 2\,\omega_{pl}(n), \quad \mathrm{Im}p_1^L(n) = -\,\gamma_1^L\omega_{pl}(n), \tag{12}$$

with the proportionality parameter γ_1^L. Given Eq. (12), $C_1^L(n)$ is uniquely determined by the sum rule in Eq. (2) and the infrared asymptotics of the kernel,

$$-\,\mathrm{Im}\frac{C_1^L(n)}{p_1^L(n)} = \lim_{\omega\to 0}\frac{\mathrm{Im}f_{xc}^L(n,\omega)}{\omega}. \tag{13}$$

The right-hand side of (13) can be evaluated from the perturbation theory [75] which predicts a small but nonzero tangent of $\mathrm{Im}f_{xc}^L(n,\omega)$ at $\omega = 0$. The frequency dependence of the OMXC kernel (12) is shown in Fig. 1 alongside the standard parametrizations of Conti-Nifosi-Tosi [72,74] (CNT) and Qian-Vignale [75] (QV). Note, that the single-oscillator OMXC kernel in Fig. 1 at $\gamma_1^L = 1$ is intermediate between the CNT and QV parametrizations. Despite its simplicity, our single-oscillator OMXC kernel correctly describes the low-frequency asymptotics and the qualitative features at the double plasmon frequency predicted earlier [72,74].

We verify the performance of our TDCDFT-OMXC approach with the kernel (12) on a benchmark problem of intersubband excitations in a $GaAs/Al_{0.3}Ga_{0.7}As$ quantum well [77,79]. Our calculations in the linear regime are consistent with the linear response theory of Ref. [77]: the value for the mode frequency 10.23 ± 0.02 meV obtained using the TDCDFT-OMXC in the linear regime agrees well with the results in Ref. [77]. In our calculations of the nonlinear dynamics we assumed that the initial state of the system is its ground state in the electric field 0.5 mV/nm. At $t = 0$ the electric field is switched off and the electron liquid in the

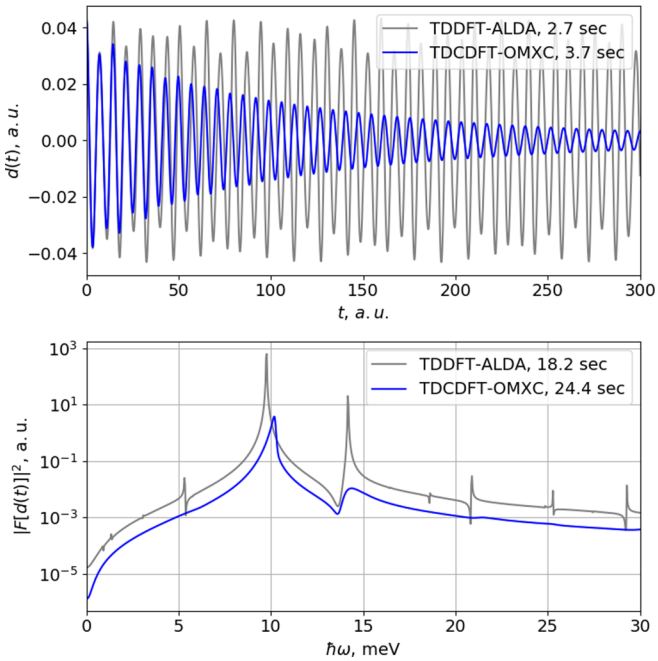

FIG. 2. Performance of the TDCDFT-OMXC (blue line) applied to calculate the nonlinear dynamics of the dipole moment in the $GaAs/Al_{0.3}Ga_{0.7}As$ quantum well, in comparison to the standard TDDFT-ALDA (gray line). The spectrum (lower panel) is calculated for the time evolution of the dipole moment during 2000 a.u. The indicated mean computation time is measured in a serial run on a single core of an Intel i7 processor.

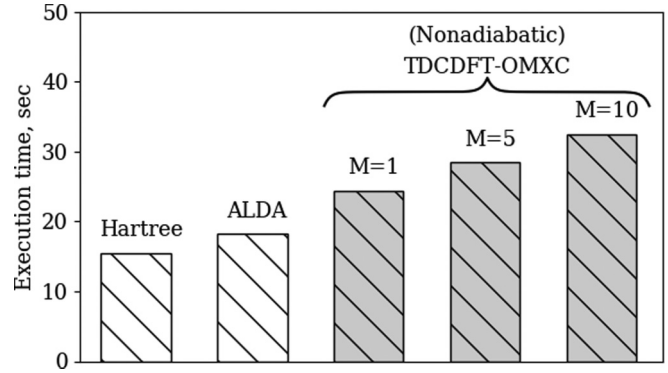

FIG. 3. The mean computation time required to propagate the electron density in a $GaAs/Al_{0.3}Ga_{0.7}As$ quantum well from $t = 0$ to 2000 a.u. with time step 0.02 a.u. The first two columns correspond to the Hartree and ALDA calculations, whereas the last three are our TDCDFT-OMXC implementation using kernels (1) with different M. The overhead due to the account of nonadiabatic effects using the single-oscillator kernel is about 35% of the time required for the ALDA calculation. The benchmarks were obtained for serial execution on a single core of an Intel i7 processor.

quantum well evolves freely in time, as seen in the evolution of the dipole moment $d(t)$ presented in Fig. 2. As seen from the figure, the velocity and the memory dependence of the effective potential of the Kohn-Sham equation result in a dissipative dynamics associated with energy relaxation [84]. In contrast, the ALDA in which all memory effects are neglected, yields a dramatically different result: the oscillations persist indefinitely without decay. The arising spectrum of frequencies associated with the nonlinear evolution is shown in the lower panel of Fig. 2. The most remarkable is the computational costs at which our nonadiabatic results were obtained: the computing time using the TDCDFT-OMXC is only about 35% larger than the time required to propagate the electron density using the standard TDDFT-ALDA [85]. In contrast, the brute-force approach with the direct evaluation of the memory integrals in Eq. (3) takes an incomparably longer time, exceeding the timing of ALDA calculation by few orders of magnitude. Further studies of intersubband excitations are provided in the Supplemental Material [86].

In our derivation of the single-oscillator kernel (12) we ignored the high-frequency asymptotics, which is a valid assumption for the low-frequency dynamics, $\omega < E_F$, where E_F is the Fermi energy. It is also possible to construct OMXC kernels valid in the entire frequency range. Indeed, while formally the OMXC can never satisfy the exact high-frequency asymptotics $\mathrm{Im} f_{xc}(n, \omega) \sim \omega^{-3/2}$ [68,87,88], in practice, the frequency range of interest is always limited from above by a finite value. Therefore, it is possible to construct an approximation to the exact high-frequency xc kernel using a finite number of oscillators in the OMXC. In the Supplemental Material [86] we provide an example of a three-oscillator OMXC kernel which satisfies the high-frequency asymptotics up to frequencies $100E_F$ with the relative error below 1%.

Because constructing more precise xc kernels will likely involve $M > 1$ contributing terms in Eq. (1), we analyze how our TDCDFT-OMXC approach scales with the number of oscillators. The computing time required to simulate the nonlinear dynamics of electron liquid in the $GaAs/Al_{0.3}Ga_{0.7}As$ quantum well using kernels with different values of M is shown in Fig. 3 alongside performances of the bare Hartree and TDDFT-ALDA. Note that the execution time grows relatively slowly with M, so that even the sophisticated ten-oscillator OMXC kernel can be used in the nonadiabatic calculations at the computational cost of only twice the timing of the standard TDDFT-ALDA.

To conclude, we propose a computationally efficient approach to the TDCDFT which enables one to replace the costly memory integrals over the whole previous time evolution with auxiliary differential equations, thereby diminishing the computational costs to that of the standard TDDFT-ALDA calculation. In addition, the OMXC kernels used in our approach have a number of useful properties: they are defined in the whole complex frequency plane, satisfy the causality, give an explicit expression for the real and imaginary parts, and have an intuitively transparent structure familiar from the standard theory of optical response. We expect that our TDCDFT-OMXC approach will open exciting opportunities for solving computationally prohibitive tasks in quantum chemistry and solid state physics beyond the ALDA.

The work is supported by the Russian Science Foundation under Grant No. 18-12-00429. The authors would like to thank Ilya Tokatly for helpful discussions.

[1] E. Runge and E. K. U. Gross, Density-Functional Theory for Time-Dependent Systems, Phys. Rev. Lett. **52**, 997 (1984).

[2] S. Botti, A. Schindlmayr, R. D. Sole, and L. Reining, Time-dependent density-functional theory for extended systems, Rep. Prog. Phys. **70**, 357 (2007).

[3] M. Casida and M. Huix-Rotllant, Progress in time-dependent density-functional theory, Annu. Rev. Phys. Chem. **63**, 287 (2012).

[4] C. A. Ullrich and Z.-h. Yang, A brief compendium of time-dependent density functional theory, Braz. J. Phys. **44**, 154 (2014).

[5] N. T. Maitra, Perspective: Fundamental aspects of time-dependent density functional theory, J. Chem. Phys. **144**, 220901 (2016).

[6] M. Marques, N. T. Maitra, F. M. S. Nogueira, E. K. U. Gross, and A. Rubio, *Fundamentals of Time-Dependent Density Functional Theory*, Lecture Notes in Physics (Springer, New York, 2012), Vol. 837.

[7] C. Ullrich, *Time-Dependent Density-Functional Theory: Concepts and Applications*, Oxford Graduate Texts (Oxford University Press, New York, 2012).

[8] Y. Takimoto, F. D. Vila, and J. J. Rehr, Real-time time-dependent density functional theory approach for frequency-dependent nonlinear optical response in photonic molecules, J. Chem. Phys. **127**, 154114 (2007).

[9] K. Lopata and N. Govind, Modeling fast electron dynamics with real-time time-dependent density functional theory: Application to small molecules and chromophores, J. Chem. Theory Comput. **7**, 1344 (2011).

[10] K. Yabana, T. Sugiyama, Y. Shinohara, T. Otobe, and G. F. Bertsch, Time-dependent density functional theory for strong electromagnetic fields in crystalline solids, Phys. Rev. B **85**, 045134 (2012).

[11] A. Castro, J. Werschnik, and E. K. U. Gross, Controlling the Dynamics of Many-Electron Systems from First Principles: A Combination of Optimal Control and Time-Dependent Density-Functional Theory, Phys. Rev. Lett. **109**, 153603 (2012).

[12] S. Meng and E. Kaxiras, Real-time, local basis-set implementation of time-dependent density functional theory for excited state dynamics simulations, J. Chem. Phys. **129**, 054110 (2008).

[13] M. Schultze, K. Ramasesha, C. D. Pemmaraju, S. A. Sato, D. Whitmore, A. Gandman, J. S. Prell, L. J. Borja, D. Prendergast, K. Yabana, D. M. Neumark, and S. R. Leone, Attosecond band-gap dynamics in silicon, Science **346**, 1348 (2014).

[14] G. Bao, G. Hu, and D. Liu, Real-time adaptive finite element solution of time-dependent Kohn-Sham equation, J. Comput. Phys. **281**, 743 (2015).

[15] K. Krieger, J. K. Dewhurst, P. Elliott, S. Sharma, and E. K. U. Gross, Laser-induced demagnetization at ultrashort time scales: Predictions of TDDFT, J. Chem. Theory Comput. **11**, 4870 (2015).

[16] M. R. Provorse and C. M. Isborn, Electron dynamics with real-time time-dependent density functional theory, Int. J. Quant. Chem. **116**, 739 (2016).

[17] N. Tancogne-Dejean, O. D. Mücke, F. X. Kärtner, and A. Rubio, Ellipticity dependence of high-harmonic generation in solids originating from coupled intraband and interband dynamics, Nat. Commun. **8**, 745 (2017).

[18] N. Tancogne-Dejean, O. D. Mücke, F. X. Kärtner, and A. Rubio, Impact of the Electronic Band Structure in High-Harmonic Generation Spectra of Solids, Phys. Rev. Lett. **118**, 087403 (2017).

[19] C. Pemmaraju, F. Vila, J. Kas, S. Sato, J. Rehr, K. Yabana, and D. Prendergast, Velocity-gauge real-time TDDFT within a numerical atomic orbital basis set, Comput. Phys. Commun. **226**, 30 (2018).

[20] N. Tancogne-Dejean and A. Rubio, Atomic-like high-harmonic generation from two-dimensional materials, Sci. Adv. **4**, eaao5207 (2018).

[21] D. C. Yost, Y. Yao, and Y. Kanai, Propagation of maximally localized Wannier functions in real-time TDDFT, J. Chem. Phys. **150**, 194113 (2019).

[22] D. C. Yost and Y. Kanai, Electronic excitation dynamics in DNA under proton and α-particle irradiation, J. Am. Chem. Soc. **141**, 5241 (2019).

[23] J. M. Soler, E. Artacho, J. D. Gale, A. García, J. Junquera, P. Ordejón, and D. Sánchez-Portal, The SIESTA method for *ab initio* order-*N* materials simulation, J. Phys.: Condens. Matter **14**, 2745 (2002).

[24] A. Schleife, E. W. Draeger, Y. Kanai, and A. A. Correa, Plane-wave pseudopotential implementation of explicit integrators for time-dependent Kohn-Sham equations in large-scale simulations, J. Chem. Phys. **137**, 22A546 (2012).

[25] M. Walter, H. Häkkinen, L. Lehtovaara, M. Puska, J. Enkovaara, C. Rostgaard, and J. J. Mortensen, Time-dependent density-functional theory in the projector augmented-wave method, J. Chem. Phys. **128**, 244101 (2008).

[26] X. Andrade, D. Strubbe, U. De Giovannini, A. H. Larsen, M. J. T. Oliveira, J. Alberdi-Rodriguez, A. Varas, I. Theophilou, N. Helbig, M. J. Verstraete, L. Stella, F. Nogueira, A. Aspuru-Guzik, A. Castro, M. A. L. Marques, and A. Rubio, Real-space grids and the Octopus code as tools for the development of new simulation approaches for electronic systems, Phys. Chem. Chem. Phys. **17**, 31371 (2015).

[27] M. Noda, S. A. Sato, Y. Hirokawa, M. Uemoto, T. Takeuchi, S. Yamada, A. Yamada, Y. Shinohara, M. Yamaguchi, K. Iida, I. Floss, T. Otobe, K.-M. Lee, K. Ishimura, T. Boku, G. F. Bertsch, K. Nobusada, and K. Yabana, SALMON: Scalable ab-initio light-matter simulator for optics and nanoscience, Comput. Phys. Commun. **235**, 356 (2019).

[28] A. K. Dhara and S. K. Ghosh, Density-functional theory for time-dependent systems, Phys. Rev. A **35**, 442 (1987).

[29] S. K. Ghosh and A. K. Dhara, Density-functional theory of many-electron systems subjected to time-dependent electric and magnetic fields, Phys. Rev. A **38**, 1149 (1988).

[30] G. Vignale and W. Kohn, Current-Dependent Exchange-Correlation Potential for Dynamical Linear Response Theory, Phys. Rev. Lett. **77**, 2037 (1996).

[31] G. Vignale, C. A. Ullrich, and S. Conti, Time-Dependent Density-Functional Theory Beyond the Local-Density Approximation, Phys. Rev. Lett. **79**, 4878 (1997).

[32] C. A. Ullrich and G. Vignale, Time-dependent current-density-functional theory for the linear response of weakly disordered systems, Phys. Rev. B **65**, 245102 (2002).

[33] J. F. Dobson, M. J. Bünner, and E. K. U. Gross, Time-Dependent Density Functional Theory beyond Linear Response: An Exchange-Correlation Potential with Memory, Phys. Rev. Lett. **79**, 1905 (1997).

[34] I. V. Tokatly, Quantum many-body dynamics in a Lagrangian frame: I. Equations of motion and conservation laws, Phys. Rev. B **71**, 165104 (2005).
[35] I. V. Tokatly, Quantum many-body dynamics in a Lagrangian frame: II. Geometric formulation of time-dependent density functional theory, Phys. Rev. B **71**, 165105 (2005).
[36] I. V. Tokatly, Time-dependent deformation functional theory, Phys. Rev. B **75**, 125105 (2007).
[37] L. Reining, V. Olevano, A. Rubio, and G. Onida, Excitonic Effects in Solids Described by Time-Dependent Density-Functional Theory, Phys. Rev. Lett. **88**, 066404 (2002).
[38] A. Marini, R. Del Sole, and A. Rubio, Bound Excitons in Time-Dependent Density-Functional Theory: Optical and Energy-Loss Spectra, Phys. Rev. Lett. **91**, 256402 (2003).
[39] R. Del Sole, G. Adragna, V. Olevano, and L. Reining, Long-range behavior and frequency dependence of exchange-correlation kernels in solids, Phys. Rev. B **67**, 045207 (2003).
[40] F. Sottile, V. Olevano, and L. Reining, Parameter-Free Calculation of Response Functions in Time-Dependent Density-Functional Theory, Phys. Rev. Lett. **91**, 056402 (2003).
[41] S. Botti, A. Fourreau, F. Nguyen, Y.-O. Renault, F. Sottile, and L. Reining, Energy dependence of the exchange-correlation kernel of time-dependent density functional theory: A simple model for solids, Phys. Rev. B **72**, 125203 (2005).
[42] P. E. Trevisanutto, A. Terentjevs, L. A. Constantin, V. Olevano, and F. D. Sala, Optical spectra of solids obtained by time-dependent density functional theory with the jellium-with-gap-model exchange-correlation kernel, Phys. Rev. B **87**, 205143 (2013).
[43] M. Gatti, Design of effective kernels for spectroscopy and molecular transport: Time-dependent current-density-functional theory, J. Chem. Phys. **134**, 084102 (2011).
[44] J. A. Berger, Fully Parameter-Free Calculation of Optical Spectra for Insulators, Semiconductors, and Metals from a Simple Polarization Functional, Phys. Rev. Lett. **115**, 137402 (2015).
[45] A. V. Terentjev, L. A. Constantin, and J. M. Pitarke, Gradient-dependent exchange-correlation kernel for materials optical properties, Phys. Rev. B **98**, 085123 (2018).
[46] D. D'Alessandro, *Introduction to Quantum Control and Dynamics* (Chapman & Hall/CRC, London, 2007).
[47] C. Brif, R. Chakrabarti, and H. Rabitz, Control of quantum phenomena: Past, present and future, New J. Phys. **12**, 075008 (2010).
[48] P. Doria, T. Calarco, and S. Montangero, Optimal Control Technique for Many-Body Quantum Dynamics, Phys. Rev. Lett. **106**, 190501 (2011).
[49] N. T. Maitra, F. Zhang, R. J. Cave, and K. Burke, Double excitations within time-dependent density functional theory linear response, J. Chem. Phys. **120**, 5932 (2004).
[50] F. Zhang and K. Burke, Adiabatic connection for near degenerate excited states, Phys. Rev. A **69**, 052510 (2004).
[51] O. V. Gritsenko and E. J. Baerends, Double excitation effect in non-adiabatic time-dependent density functional theory with an analytic construction of the exchange-correlation kernel in the common energy denominator approximation, Phys. Chem. Chem. Phys. **11**, 4640 (2009).
[52] P. Romaniello, D. Sangalli, J. A. Berger, F. Sottile, L. G. Molinari, L. Reining, and G. Onida, Double excitations in finite systems, J. Chem. Phys. **130**, 044108 (2009).
[53] D. Sangalli, P. Romaniello, G. Onida, and A. Marini, Double excitations in correlated systems: A many-body approach, J. Chem. Phys. **134**, 034115 (2011).
[54] N. Säkkinen, M. Manninen, and R. van Leeuwen, The Kadanoff-Baym approach to double excitations in finite systems, New J. Phys. **14**, 013032 (2012).
[55] K. S. Novoselov, A. Mishchenko, A. Carvalho, and A. H. Castro Neto, 2D materials and van der Waals heterostructures, Science **353**, aac9439 (2016).
[56] J. C. Blancon, H. Tsai, W. Nie, C. C. Stoumpos, L. Pedesseau, C. Katan, M. Kepenekian, C. M. M. Soe, K. Appavoo, M. Y. Sfeir, S. Tretiak, P. M. Ajayan, M. G. Kanatzidis, J. Even, J. J. Crochet, and A. D. Mohite, Extremely efficient internal exciton dissociation through edge states in layered 2D perovskites, Science **355**, 1288 (2017).
[57] P. Rivera, K. L. Seyler, H. Yu, J. R. Schaibley, J. Yan, D. G. Mandrus, W. Yao, and X. Xu, Valley-polarized exciton dynamics in a 2D semiconductor heterostructure, Science **351**, 688 (2016).
[58] X.-X. Zhang, Y. You, Shu Yang Frank Zhao, and T. F. Heinz, Experimental Evidence for Dark Excitons in Monolayer WSe_2, Phys. Rev. Lett. **115**, 257403 (2015).
[59] A. Chernikov, A. M. van der Zande, H. M. Hill, A. F. Rigosi, A. Velauthapillai, J. Hone, and T. F. Heinz, Electrical Tuning of Exciton Binding Energies in Monolayer WS_2, Phys. Rev. Lett. **115**, 126802 (2015).
[60] V. Turkowski, A. Leonardo, and C. A. Ullrich, Time-dependent density-functional approach for exciton binding energies, Phys. Rev. B **79**, 233201 (2009).
[61] J. A. Berger, P. Romaniello, R. van Leeuwen, and P. L. de Boeij, Performance of the Vignale-Kohn functional in the linear response of metals, Phys. Rev. B **74**, 245117 (2006).
[62] M. Van Faassen, Time-dependent Current-density-functional theory applied to atoms and molecules, Int. J. Mod. Phys. A **20**, 3419 (2006).
[63] J. A. Berger, P. L. de Boeij, and R. van Leeuwen, Analysis of the Vignale-Kohn current functional in the calculation of the optical spectra of semiconductors, Phys. Rev. B **75**, 035116 (2007).
[64] C. A. Ullrich and I. V. Tokatly, Nonadiabatic electron dynamics in time-dependent density-functional theory, Phys. Rev. B **73**, 235102 (2006).
[65] C. A. Ullrich, Time-dependent density-functional theory beyond the adiabatic approximation: Insights from a two-electron model system, J. Chem. Phys. **125**, 234108 (2006).
[66] J. M. Escartín, M. Vincendon, P. Romaniello, P. M. Dinh, P.-G. Reinhard, and E. Suraud, Towards time-dependent current-density-functional theory in the non-linear regime, J. Chem. Phys. **142**, 084118 (2015).
[67] P. M. Dinh, L. Lacombe, P.-G. Reinhard, É. Suraud, and M. Vincendon, On the inclusion of dissipation on top of mean-field approaches, Eur. Phys. J. B **91**, 246 (2018).
[68] E. K. U. Gross and W. Kohn, Local Density-Functional Theory of Frequency-Dependent Linear Response, Phys. Rev. Lett. **55**, 2850 (1985).
[69] R. C. Ball, C. T. Coffin, H. R. Gustafson, L. W. Jones, M. J. Longo, T. J. Roberts, B. P. Roe, E. Wang, C. Castoldi, G. Conforto, M. B. Crisler, J. S. Hoftun, T. Y. Ling, T. A. Romanowski, J. T. Volk, S. Childress, M. E. Duffy, G. K. Fanourakis, R. J. Loveless, D. D. Reeder, D. L. Schumann,

and E. S. Smith, Prompt Muon-Neutrino Production in a 400-GeV Proton Beam-Dump Experiment, Phys. Rev. Lett. **57**, 923 (1986).

[70] N. Iwamoto and E. K. U. Gross, Correlation effects on the third-frequency-moment sum rule of electron liquids, Phys. Rev. B **35**, 3003 (1987).

[71] H. M. Böhm, S. Conti, and M. P. Tosi, Plasmon dispersion and dynamic exchange-correlation potentials from two-pair excitations in degenerate plasmas, J. Phys.: Condens. Matter **8**, 781 (1996).

[72] S. Conti, R. Nifosí, and M. P. Tosi, The exchange-correlation potential for current-density functional theory of frequency-dependent linear response, J. Phys.: Condens. Matter **9**, L475 (1997).

[73] R. Nifosí, S. Conti, and M. Tosi, Dynamic exchange-correlation potentials for the 2D electron gas, Physica E (Amsterdam, Neth.) **1**, 188 (1997).

[74] R. Nifosí, S. Conti, and M. P. Tosi, Dynamic exchange-correlation potentials for the electron gas in dimensionality $D = 3$ and $D = 2$, Phys. Rev. B **58**, 12758 (1998).

[75] Z. Qian and G. Vignale, Dynamical exchange-correlation potentials for an electron liquid, Phys. Rev. B **65**, 235121 (2002).

[76] H. Haug and S. W. Koch, *Quantum Theory of the Optical and Electronic Properties of Semiconductors*, 4th ed. (World Scientific, Singapore, 2004).

[77] C. A. Ullrich and G. Vignale, Collective intersubband transitions in quantum wells: A comparative density-functional study, Phys. Rev. B **58**, 15756 (1998).

[78] S. Groth, T. Dornheim, and J. Vorberger, *Ab initio* path integral Monte Carlo approach to the static and dynamic density response of the uniform electron gas, Phys. Rev. B **99**, 235122 (2019).

[79] H. O. Wijewardane and C. A. Ullrich, Time-Dependent Kohn-Sham Theory with Memory, Phys. Rev. Lett. **95**, 086401 (2005).

[80] Y. Kurzweil and R. Baer, Quantum memory effects in the dynamics of electrons in gold clusters, Phys. Rev. B **73**, 075413 (2006).

[81] A. Odintsov, V. Semenov, and A. Zorin, Specific problems of numerical analysis of the Josephson junction circuits, IEEE Trans. Magn. **23**, 763 (1987).

[82] D. R. Gulevich, V. P. Koshelets, and F. V. Kusmartsev, Josephson flux-flow oscillator: The microscopic tunneling approach, Phys. Rev. B **96**, 024515 (2017).

[83] K. S. Singwi, M. P. Tosi, R. H. Land, and A. Sjölander, Electron Correlations at Metallic Densities, Phys. Rev. **176**, 589 (1968).

[84] R. D'Agosta and G. Vignale, Relaxation in Time-Dependent Current-Density-Functional Theory, Phys. Rev. Lett. **96**, 016405 (2006).

[85] To obtain the results presented in Fig. 2 we used the single-oscillator kernel given by Eqs. (12) assuming zero tangent of $\mathrm{Im} f_{xc}^{L}(n, \omega)$ at $\omega = 0$ in Eq. (13). The use of the exact tangent (13) from the perturbation theory [75] takes about 30% longer execution time, but has no observable effects on the dynamics of the quantum well as compared to the simpler version of the kernel.

[86] See Supplemental Material at http://link.aps.org/supplemental/10.1103/PhysRevB.100.241109 for further details on the derivation of OMXC kernels and benchmarks of the TDCDFT-OMXC approach.

[87] A. Holas and K. S. Singwi, High-frequency damping of collective excitations in fermion systems. I. Plasmon damping and frequency-dependent local-field factor in a two-dimensional electron gas, Phys. Rev. B **40**, 158 (1989).

[88] A. J. Glick and W. F. Long, High-frequency damping in a degenerate electron gas, Phys. Rev. B **4**, 3455 (1971).